Chemical Science

ROYAL SOCIETY OF CHEMISTRY

EDGE ARTICLE

View Article Online
View Journal | View Issue

Cite this: *Chem. Sci.*, 2021, **12**, 13580

All publication charges for this article have been paid for by the Royal Society of Chemistry

Boosting purely organic room-temperature phosphorescence performance through a host–guest strategy†

Mengke Li,[a] Xinyi Cai,[a] Zijian Chen,[a] Kunkun Liu,[ab] Weidong Qiu,[a] Wentao Xie,[a] Liangying Wang[a] and Shi-Jian Su *[ab]

Received 23rd June 2021
Accepted 19th September 2021

DOI: 10.1039/d1sc03420k

rsc.li/chemical-science

The host–guest doping system has aroused great attention due to its promising advantage in stimulating bright and persistent room-temperature phosphorescence (RTP). Currently, exploration of the explicit structure–property relationship of bicomponent systems has encountered obstacles. In this work, two sets of heterocyclic isomers showing promising RTP emissions in the solid state were designed and synthesized. By encapsulating these phosphors into a robust phosphorus-containing host, several host–guest cocrystalline systems were further developed, achieving highly efficient RTP performance with a phosphorescence quantum efficiency (ϕ_P) of ~26% and lifetime (τ_P) of ~32 ms. Detailed photophysical characterization and molecular dynamics (MD) simulation were conducted to reveal the structure–property relationships in such bicomponent systems. It was verified that other than restricting the molecular configuration, the host matrix could also dilute the guest to avoid concentration quenching and provide an external heavy atom effect for the population of triplet excitons, thus boosting the RTP performance of the guest.

Introduction

Many studies on room-temperature phosphorescence (RTP) materials have been conducted owing to their attractive applications in the field of anti-counterfeiting,[1–3] biological imaging free of background autofluorescence interference,[4–6] and flexible electroluminescence.[7–10] Despite wide application of precious-noble-metal-containing phosphorescent materials in display and lighting,[9,11] RTP emission from purely organic materials still faces great challenges of vulnerable long-lived triplet excitons. In light of some unique advantages, such as low-cost, no biological toxicity and easier processing, diverse design strategies have been applied to develop purely organic RTP materials, mainly due to the consideration of enhancing the spin–orbit coupling (SOC) interaction and inhibiting nonradiative deactivation.[12–18] In general, strong intermolecular interactions are favoured for both stabilizing triplet excitons and restricting intra- and intermolecular motions, thus conducive to effective phosphorescence emission.[18–20] Currently, crystallization-induced phosphorescence is the greatest concern in developing efficient RTP systems, including single-component molecular crystals and host–guest cocrystals.[21–26]

In the solid state, a variety of single-component RTP materials composed of some traditional organic functional groups, such as carbazole,[23,27,28] halogen elements,[29,30] aromatic carbonyl groups and so on have been successfully established.[3,22,31] Compared with these single-component RTP materials, host–guest chemistry has received increasing attention because of its ability to boost phosphorescence performance through some distinctive characters of the host matrix. Recently, a number of favourable host materials have been developed, including macrocyclic compounds,[32] polymer matrices,[33–35] and co-crystallized organic small molecular hosts.[36–39] Among them, the host–guest cocrystal matrix has been carefully studied because its powerful crystalline lattice can protect the guest from quenched species such as water, oxygen and other nonradiative factors.[15,40] Despite the progress made in the host–guest chemistry, the investigation of a specific clustered structure still encounters many obstacles due to the lack of the cocrystal structure, especially when the guest content is very low. Currently, limited cluster-state structural analyses have been reported, so the exploration of the luminescence mechanism is still insufficient. Meanwhile, for most cocrystalline host and guest compounds, specific functional groups such as heavy halogen atoms, carbazole or aromatic carbonyl are utilized, providing vast space for further exploration considering a huge organic library.[24,41] Consequently, developing

[a]*State Key Laboratory of Luminescent Materials and Devices and Institute of Polymer Optoelectronic Materials and Devices, South China University of Technology, Guangzhou 510640, P. R. China. E-mail: mssjsu@scut.edu.cn*

[b]*South China Institute of Collaborative Innovation, Dongguan 523808, China*

† Electronic supplementary information (ESI) available. CCDC 2091741 and 2091742. For ESI and crystallographic data in CIF or other electronic format see DOI: 10.1039/d1sc03420k

promising host–guest RTP materials and carrying out accurate bicomponent conformation investigation are still in demand.

In light of the unique advantages of the host in activating persistent RTP, we hypothesized an efficient host–guest RTP system through effective molecular design strategies. In this regard, we first set out to develop an efficient guest which served as the RTP center. In our previous work, it has been proved that phenoxathiine and thianthrene show promising RTP emission.[42] Based on this, two sets of isomeric phenoxathiine and thianthrene derivatives were designed and synthesized, as shown in Fig. 1. The heteroatoms N, O and S featuring n–π* transition characteristics can enhance singlet–triplet SOC interactions as indicated by El-Sayed rules, making these heterocyclic building blocks promising RTP candidates.[18,43] After the 1(1′) or 2(2′) position of phenoxathiine and thianthrene is replaced by the heteroatom N by connecting adjacent phenyl groups, these structures are endowed with different intra- and/or intermolecular hydrogen bond (H-bond) interactions. The position 1(1′) substituted 12H- isomers tend to form close intramolecular H-bond interactions (N–H···S or N–H···O), whereas the N–H bond of 5H- isomers can interact with the heteroatoms of the surrounding molecules in the aggregated state to form dense intermolecular H-bonds. These H-bonds contribute to restrict molecular motions and thus attenuate the vibrational dissipation of triplet excitons.[44,45] All these compounds exhibit RTP emissions through this effective molecular design strategy. Also, the different effects of intra and intermolecular H-bonds on regulating phosphorescence properties were further revealed *via* isomer engineering. It is worth noting that the planar π-conjugated characteristics of these structures make them susceptible to concentration quenching upon aggregation. Inspired by host–guest chemistry, to boost RTP performance, a promising phosphorus-containing host, 1,2-bis(diphenylphosphino)ethane (DIPHOS), is further developed to dilute these isomers while providing a robust environment to confine the molecular configuration. By encapsulating these phosphors into the powerful crystalline host, the resulting host–guest cocrystalline systems realize more efficient and persistent RTP performance in contrast to single-component molecular crystals. Unlike single-component RTP materials, it is very difficult to obtain the single crystal structure of bicomponent co-crystal systems. Also, the doping ratio of the host to the guest in the co-crystal obtained from the solution mixture is always inconsistent with the initial raw ratio. Herein, we provide a method to investigate the aggregated structure of the host–guest system. The doping concentration of the guest is experimentally confirmed, followed by a molecular dynamics (MD) simulation to simulate the aggregated morphologies. Thereafter, further experimental analyses and theoretical calculations are conducted to demonstrate the greatly elevated phosphorescence performance in such host–guest systems.

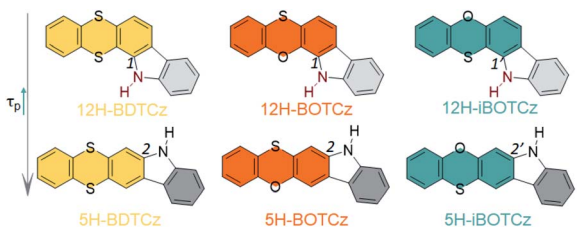

Fig. 1 Molecular structures of the investigated guest compounds.

Results and discussion

UV-vis absorption and photoluminescence (PL) spectra in dilute chloroform solutions (10^{-5} M) are shown to illustrate the luminescence properties of the guests in the isolated state (Fig. S1 and S2†). Vulnerable to the attacks of molecular vibrations, structural relaxation and multiple active quenchers, all compounds exhibit only fluorescence emissions at around 400 nm. 12H-BDTCz and 5H-BDTCz exhibit slightly bathochromic fluorescence emissions due to their larger configuration relaxation in excited states. The degree of configuration relaxation can be interpreted from the value of root-mean square displacement (RMSD), which represents the geometry changes in the ground state and excited state. These significant RMSD values of these structures shown in Fig. S23† imply non-negligible vibrational relaxation losses in the isolated state. So, constructing a rigid matrix to confine the molecular geometry so that triplet excitons can be free of both internal and external attacks is critical.

In view of this, the luminescent properties of these compounds in the solid state were examined, indicating that they all achieved phosphorescence emissions in millisecond lifetime at room temperature. Temperature-dependent PL spectra further confirm their phosphorescence properties through significantly increased PL intensity as the temperature decreases (Fig. S4 and S9†). The phosphorescence spectra are blue-shifted with decreasing temperature, which can be attributed to the suppressed configuration relaxation at low temperatures.[42] The structural features of fluorescence and phosphorescence can be attributed to the transitions of the molecular vibrational levels. It is noteworthy that the phosphorescence performance of 5H-BDTCz, 5H-BOTCz and 5H-iBOTCz is at variance with their respective 12H-isomers. As monitored by using steady-state PL profiles and transient PL decay curves, 5H-structures present better phosphorescence properties, including elevated phosphorescence intensity and longer afterglow lifetime, indicating both effective ISC and phosphorescence radiation processes for 5H-isomers (Fig. 2, S7 and S8†). To interpret the different solid-state luminescence properties regulated by isomer engineering, a systematic analysis on molecular packing mode is a requisite.

Taking isomeric thianthrene derivatives 12H-BDTCz and 5H-BDTCz as examples, initially, orderly stacked crystal structures were grown from saturated ethanol solutions followed by the X-ray diffraction experiment to explore specific molecular interactions. Detailed photo-physical characterization of crystals and computation simulations were then performed to reveal the underlying phosphorescence mechanism. The single crystal unit cells and adjacent dimers were extracted from single crystal structures (Fig. 3c). Remarkably, there exists a N–H···S distance of 4.323 Å in the 12H-BDTCz crystal, which is a long-range

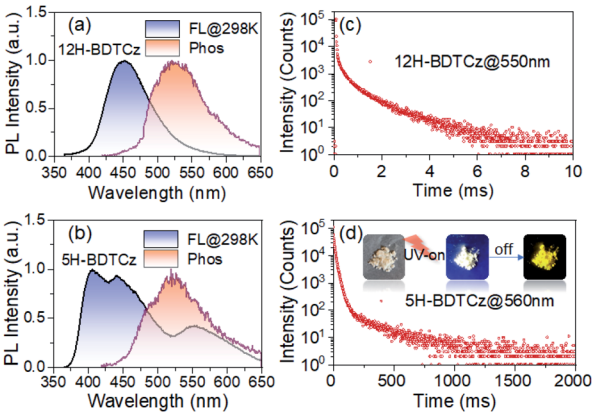

Fig. 2 Steady-state PL and phosphorescence spectra (blue areas for fluorescence emission measured at 298 K, and orange areas for phosphorescence emission detected at 77 K with 50 ms time delay) of (a) 12H-BDTCz and (b) 5H-BDTCz in crystalline states, and corresponding phosphorescence transient decay curves of (c) 12H-BDTCz and (d) 5H-BDTCz.

interaction compared with that of 5H-DBTCz (3.767 Å). In contrast, a closer intramolecular N–H···S contact of 2.957 Å is formed in 12H-BDTCz. Thereof, a denser intermolecular packing is observed in 5H-BDTCz which is consistent with its much higher crystal density of 1.514 g cm^{-3} than that of 12H-BDTCz (1.439 g cm^{-3}). It is well established that for phosphorescence processes, effective intermolecular interactions are more conducive to the suppression of non-radiative losses caused by vibration and quencher permeation.[46,47] Further, to better reveal the electronic nature of excited states in the solid state, hybrid quantum mechanics and molecular mechanics (QM/MM) calculations were performed by using a two-layer ONIOM model to reveal the role of the solid environment (Fig. 3g).[48] The central QM part is described with quantum mechanics, whereas the surrounding MM part is treated with molecular force field. The calculated energy diagrams of the excited singlet state and multiple triplet states (the energy level difference between S_1 and T_n is less than 0.3 eV) present that there exists one favorable ISC channel ($S_1 \rightarrow T_2$) for 12H-BDTCz, but an increased channel is observed for 5H-BDTCz (Fig. 3e).[49] Also, the T_2 energy level of 5H-BDTCz is lower than S_1, hence triplet excitons are more readily populated. Accordingly, the SOC matrix elements involved in these favorable ISC channels and phosphorescent radiation processes were calculated by using the Dalton package using the atomic mean field approximation approach.[50] Strikingly, all of these processes possess considerable SOC constants, indicating that strong spin–orbit interactions between states of different multiples were achieved through an effective molecular design concept. Further time-dependent density functional theory (TD-DFT) calculations also reveal that the n–π* transition nature contributes to the overall natural transition orbitals (NTOs) owing to the incorporation of heteroatoms (Fig. 3f).[51,52] Also, a relatively small SOC value between T_1 and S_0 is observed for 5H-BDTCz, which can be explained by its dominant π–π* transition character located at the carbazole fragment.[18] Overall, efficient phosphorescence emissions are achieved in the solid state, and with the N–H···S H-bond varied from favorable intramolecular interactions to close intermolecular interactions, elevated phosphorescence performance is achieved because of dense crystal packing. Accordingly, insight into the mechanism of different phosphorescence properties tuned by intra- and intermolecular hydrogen bonds was finally obtained in virtue of the molecular packing mode.

This significant effect of intra- and intermolecular H-bonds on phosphorescence properties could be further proved by investigating the luminescence properties of isomeric phenoxathiine derivatives 12H-BOTCz, 5H-BOTCz, 12H-iBOTCz and 5H-iBOTCz in the solid state. Unexpectedly, the single crystal

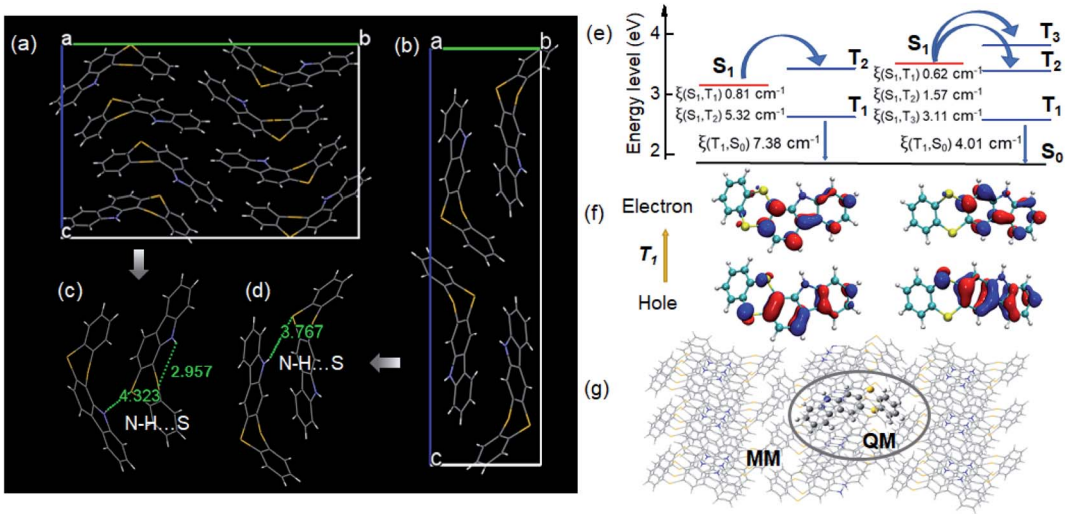

Fig. 3 Single crystal structures of (a) 12H-BDTCz and (b) 5H-BDTCz; intermolecular interactions related to the hydrogen bond of (c) 12H-BDTCz and (d) 5H-BDTCz; (e) calculated energy levels and SOC constants of 12H-BDTCz (left) and 5H-BDTCz (right) structures extracted from crystals; (f) NTOs of triplet states of 12H-BDTCz (left) and 5H-BDTCz (right); (g) selected two-layer ONIOM models used for QM/MM calculations.

structures of these four isomers were not resolved because we failed to grow their crystals. In spite of this, it is noted that these materials exhibit similar XRD patterns in crystal and powder states (Fig. S5†). So, phosphorescence properties of these four isomers were investigated in the powder state (Fig. S6†). As shown in Fig. S5 and S6,† RTP emissions were detected for 12H-BOTCz, 5H-BOTCz, 12H-iBOTCz and 5H-iBOTCz in the solid state, and phosphorescence lifetimes of 5H-BOTCz and 5H-iBOTCz are longer than that of 12H-BOTCz and 12H-iBOTCz as expected. The photo-physical experiments unambiguously indicate that their phosphorescence performance follows the same trend as that of 12H-BDTCz and 5H-BDTCz isomers, which undoubtedly further supports the above analyses.

However enhanced RTP performances are achieved for 5H-isomers *via* isomer engineering by regulating intermolecular interactions. Notably, temperature-dependent experiments indicate that the phosphorescence performance shows large potential for improvement when encapsulated in a perfect environment (Fig. S9†). Further, inspired by the concept of host–guest chemistry, it is expected that their RTP performance can be further improved by means of some unique characters of the host. Herein, a new promising host molecule DIPHOS is developed, which can better utilize triplet excitons of the guests (Fig. 4a). DIPHOS is commonly used as a reagent in a wide range of catalytic chemical reactions, and is easy to crystallize from ethanol and forms a robust matrix.[53,54] Also, the flexible ethyl chain between two phosphorus atoms endows it with promising compatibility with surrounding molecules through modulating the molecular configuration when the guests are dissolved in it. On account of this, vibrational deactivation can also be effectively suppressed by encapsulating the emitter into the host without obvious emitter aggregation. In this way, the concentration quenching effect will be well suppressed. Besides, owing to the two phosphorus atoms of the host that can provide the external heavy atom effect, the intersystem crossing efficiency can be greatly promoted through enhanced SOC interaction. As thus, greatly improved phosphorescence performance is achieved by utilizing DIPHOS as a highly rigid host skeleton. Thereafter, detailed experimental and theoretical analyses are conducted to demonstrate the in-depth RTP mechanism of this host–guest system.

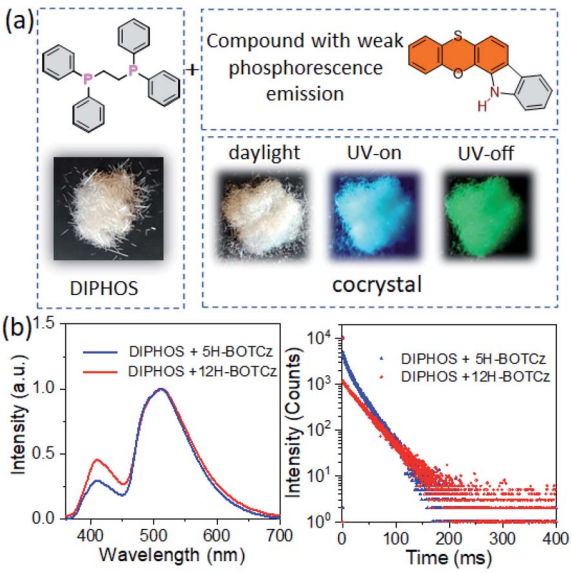

Fig. 4 (a) Proposed host–guest system. Left: structure of the host material (DIPHOS) and its crystal image; right: obtained cocrystal by dissolving 12H-BOTCz in the DIPHOS host and its photos taken before and after 365 nm UV lamp irradiation; (b) steady state photoluminescence spectra (left) and phosphorescence decay curves (right) detected at 298 K by dissolving 12H-BOTCz and 5H-BOTCz in the host matrix.

Taking 12H-BOTCz as an example, the guest and host materials were dissolved in ethanol solution at an initial molar ratio of 3 : 1, and the cocrystal was grown from this solution mixture. The above experiments indicate that 12H-BOTCz exhibits a dominant deep-blue fluorescence emission in the solid state, and the DIPHOS host is almost nonluminous with an extremely low photoluminescence quantum yield of 0.6% in the solid state. However, the resultant cocrystal exhibits sky-blue emission at a steady state and apparently homogeneous green afterglow can be observed after ceasing illumination (Fig. 4a). The cocrystal was excited at 350 nm, and at this wavelength, only the guests can be excited and the host cannot be excited (Fig. S10†). Different from the single-component crystal of 12H-BOTCz, the steady-state PL spectra of cocrystal 12H-BOTCz:DIPHOS show that the phosphorescence intensity at 450 to 600 nm is greatly elevated relative to the fluorescence intensity. Accordingly, a significant phosphorescence quantum yield of 25.6% was measured, which is more than one magnitude higher than that of the single-component crystals (less than 1%). Furthermore, a very different phosphorescence decay with a lifetime of 32 ms was also detected, which is two orders of magnitude higher than that detected in the single-component crystals of 12H-BOTCz (less than 0.1 ms) (Fig. 4b and S8a†). All the results indicate that DIPHOS can be used as a promising host matrix to boost the phosphorescence performance of the guest. The universality and significance of this host–guest strategy is further supported by dissolving 12H-BDTCz and 5H-BOTCz in the DIPHOS matrix, respectively (Fig. 4b and S12†).

Although the initial mixing molar ratio of the host to the guest is 3 : 1, it is well established that the ratio of the two in the precipitated cocrystal is always not consistent with the raw ratio. To explore the specific composition of the host–guest system, high performance liquid chromatography (HPLC) analysis was performed to probe the exact contents of the individual host and guest components. The HPLC results show that the signals of the two components, 12H-BOTCz and DIPHOS, were detected at different times. First, a small amount of the guest component was detected after 5 minutes of sample injection, which is consistent with the time when the pure guest material was detected, followed by the detection of the main signal of the host material (Fig. 5c). Accordingly, the content of the guest material in the host–guest system was identified as 4.2%, indicating that the guest component was diluted in the host matrix at a low concentration, as illustrated by the diagram in Fig. 5a. Upon carefully investigating the luminescence behavior of the individual host, guest and the cocrystal system,

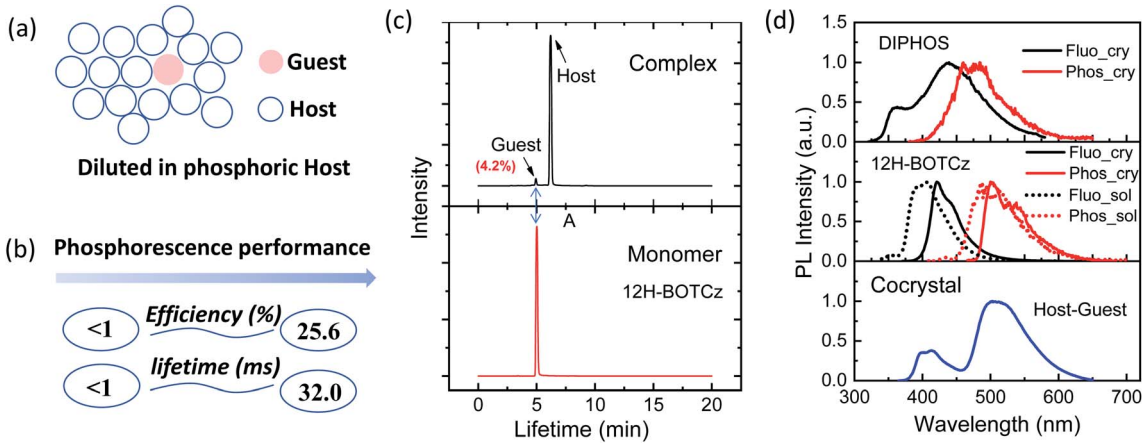

Fig. 5 (a) Graphic illustration of the host–guest system; (b) changes in phosphorescence performance after introduction of the host material; (c) HPLC analysis of the 12H-BOTCz monomer and its host–guest complex; (d) comparison of photoluminescence spectra of individual DIPHOS, 12H-BOTCz crystals and the formed host–guest systems.

it was found that the fluorescence and phosphorescence peaks of the cocrystal system are identical to the spectra of the guest recorded in dilute solution, which further confirms the proposed host–guest doping architecture. Based on the above analysis, a series of host–guest doped films were also prepared by solution processing, and the doping ratio of the host to the guest was kept to be consistent with that obtained by the HPLC experiment. For comparison, single component neat films of the guests were also prepared to confirm the positive role of the host in assisting RTP emission. The phosphorescence intensities of both neat guest films and host–guest doping films were undoubtedly reduced compared with those of crystal states due to weakened environmental rigidity (Fig. S15–S17†). Even so, a significant enhancement of the phosphorescence performance was still observed in the doped films, including both greatly enhanced phosphorescence intensity and afterglow lifetime. Besides the currently developed RTP emitters, the previously reported phenoxathiine derivatives[42] were also investigated as the guests for developing host–guest RTP systems with DIPHOS as the host. Significantly improved phosphorescence performance in comparison with that of the neat films of phenoxathiine derivatives further prove the universality of the host in assisting bright and long afterglow luminescence (Fig. S18†).

It is of great significance to clearly understand the positive roles of the host in such a bicomponent system. Here, the effect of the host is discussed based on the processes of ISC and phosphorescence radiation, which play a decisive role in defining phosphorescence performance.[12,40] Despite some studies referring to the enhancement of the heavy atom effect on SOC interaction, there is a lack of solid experimental evidence for it being difficult to eliminate the influence of the non-radiative process to discuss the ISC process. In this work, to preclude the influence of the non-radiative process, a temperature-dependent experiment of 12H-BOTCz in the solid state was conducted at extremely low temperatures from 80 K to 10 K. As shown in Fig. S10,† the fluorescence intensity is basically unchanged in this temperature range and the phosphorescence intensity shows tiny variance at the temperature near 10 K, under which condition the non-radiative decay pathways are generally believed to be well suppressed. Even so, it is noticed that the phosphorescence intensity was still very weak relative to the fluorescence emission, indicating an inadequate ISC process of the single-component molecular system. This result indicates that the external heavy atom effect must be taken into consideration to illustrate the dramatic enhancement of the phosphorescence quantum yield.

As often mentioned, the host matrix can act as a robust environment to restrict vibrations of the guest molecules, thus suppressing non-radiative decay for effective RTP emission. Besides, by dispersing trace amounts of the guest molecules into the host matrix, the host can dilute the guest emitters as a solid solvent, thus avoiding the concentration quenching effect caused by aggregation.[36,55] However, considering the low doping ratio of the guests in the host–guest system, it is much difficult to obtain a precise cocrystal structure through traditional single crystal XRD technology, limiting its further investigation. Herein, to gain a deeper understanding of the underlying mechanism and provide a solid theoretical support for the role of the host often discussed, MD calculations were conducted to simulate the aggregation structure of the host–guest system. Taking the 12H-BOTCz doped system as an example, a periodic cubic box consisting of 12H-BOTCz and DIPHOS was first constructed and their ratio was kept to be consistent with the HPLC result (Fig. 6a). Considering that the cocrystal was obtained by cooling a mixed solution from 340 K down to room temperature, a periodic heating and cooling process from 290 K to 340 K to 290 K was repeated to allow molecules to move adequately at 340 K and to replicate the actual deposition state as much as possible. The detailed annealing MD process is shown in Fig. 6c. The statistical average density of the host–guest cubic box in the simulation process is 1.12 g cm^{-3}, which is close to that of the single-component DIPHOS molecular crystal (1.23 g cm^{-3}), and the

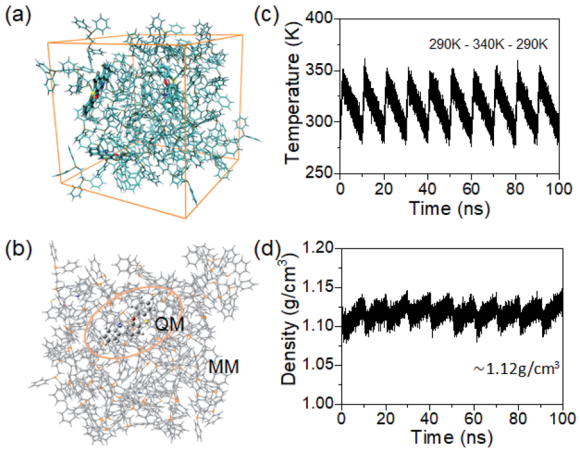

Fig. 6 (a) A cubic box consisting of 12H-BOTCz and DIPHOS structures used for MD simulation; (b) two-layer ONIOM model of host–guest clusters consisting of 12H-BOTCz and DIPHOS structures; (c) temperature program of periodic annealing of MD simulation; (d) density of the aggregates in the MD process (the calculated average density is 1.12 g cm^{-3}).

slightly reduced density may be attributed to the substitution of some small molecular weight guest molecules (Fig. 6d). After completion of the MD process, a few representative self-assembled cluster structures were selected for further analysis (Fig. S20†). In one respect, it is noticed that no aggregated guest molecular morphology is observed in any of the cluster structures, indicating that guest molecules are well distributed in the host matrix in a discrete way, thus avoiding the phosphorescence quenching caused by the aggregation of guest emitters, which is expected to be conducive to the improved phosphorescence performance to some extent. This advantage is further experimentally confirmed by detecting the luminescent properties of a series of doped films with different concentrations of the guests. As shown in Fig. S19,† the phosphorescence intensity and lifetime significantly increase with the decrease of concentration, indicating that the phosphorescence quenching caused by emitter aggregation can be effectively suppressed at a low doping concentration.

In addition, hybrid QM/MM calculations of these respective clusters were conducted by using a two-layer ONIOM model to analyze the molecular geometries of the guest in ground and excited states (Fig. 6b). The central 12H-BOTCz molecule was treated as the QM part and described with quantum mechanics, whereas the surrounding host molecules were treated as the MM part and calculated using molecular force field. To analyze the role of the host in limiting the molecular configuration relaxation and qualitatively evaluate the degree of geometry deviations, RMSD values of the excited singlet and triplet state structures relative to those of the ground state structures were calculated. The average RMSD (S_1, S_0) and RMSD (T_1, S_0) of the guest in the host–guest system were calculated to be 0.1051 and 0.1405 respectively, which are much lower than those of 12H-BOTCz in the isolated state (0.4397 and 0.5254), indicating a limited vibrational relaxation process. These results demonstrate that the rigid environment provided by the host matrix can effectively reduce the nonradiative deactivation of the guest (Fig. S21–S22†). In particular, it should be highlighted that the reliability of the analysis on aggregated structures by MD simulation is better demonstrated by the phosphorescence behavior in the amorphous doped films, as mentioned in the above analysis (Fig. S15–S18†). In summary, DIPHOS can serve as a promising host matrix through providing a powerful environment for the guest to suppress nonradiative losses.

Conclusions

In conclusion, six new compounds with weak RTP emission in the solid state were designed and synthesized. Further, different effects of intra- and intermolecular H-bonds on phosphorescence properties regulated by isomer engineering are specifically highlighted. In the aggregated state, the structure with the capability of forming a dense intermolecular hydrogen bond contact gives the best phosphorescence performance. By employing DIPHOS as a rigid host matrix, these RTP isomers exhibit brighter and longer afterglow luminescence than those in the corresponding unimolecular crystalline state. Accordingly, the positive role of the host in promoting phosphorescence performance of the guest is proved through detailed experimental analysis combined with molecular dynamics simulation. It is demonstrated that the synergistic effect of the incremental intersystem crossing process by the external heavy atom effect, inhibited multiple nonradiative deactivation processes, and suppressed concentration quenching effect induced by emitter aggregation, are responsible for the enhanced persistent phosphorescence. This work provides a deeper understanding of the phosphorescence enhancement effect of the host–guest chemistry, and a rigid phosphorus-containing host has great potential in achieving bright and persistent organic afterglow luminescence.

Data availability

Experimental supporting data are presented in the ESI.†

Author contributions

M. L. conducted the project and prepared the manuscript. M. L. and Z. C. contributed to the synthesis and characterization. W. Q., W. X. and L. W. contributed to the optical measurement. X. C. and K. L. contributed to the analyses of results. S. J. S. performed data analysis and prepared the manuscript.

Conflicts of interest

There are no conflicts to declare.

Acknowledgements

The authors greatly appreciate the financial support from the National Natural Science Foundation of China (51625301, 91833304, and 51861145301), the Basic and Applied Basic Research Foundation of Guangdong Province

(2019B1515120023), and the Guangdong Provincial Department of Science and Technology (2016B090906003 and 2016TX03C175).

Notes and references

1 W. Li, Q. Huang, Z. Mao, J. Zhao, H. Wu, J. Chen, Z. Yang, Y. Li, Z. Yang, Y. Zhang, M. P. Aldred and Z. Chi, *Angew. Chem., Int. Ed.*, 2020, **59**, 3739–3745.
2 Z. An, C. Zheng, Y. Tao, R. Chen, H. Shi, T. Chen, Z. Wang, H. Li, R. Deng, X. Liu and W. Huang, *Nat. Mater.*, 2015, **14**, 685–690.
3 Y. Lai, T. Zhu, T. Geng, S. Zheng, T. Yang, Z. Zhao, G. Xiao, B. Zou and W. Z. Yuan, *Small*, 2020, **16**, 2005035.
4 C. C. Kenry and B. Liu, *Nat. Commun.*, 2019, **10**, 2111.
5 Z. He, H. Gao, S. Zhang, S. Zheng, Y. Wang, Z. Zhao, D. Ding, B. Yang, Y. Zhang and W. Z. Yuan, *Adv. Mater.*, 2019, **31**, 1807222.
6 Q. Dang, Y. Jiang, J. Wang, J. Wang, Q. Zhang, M. Zhang, S. Luo, Y. Xie, K. Pu, Q. Li and Z. Li, *Adv. Mater.*, 2020, **32**, 2006752.
7 D. R. Lee, K. H. Lee, W. Shao, C. L. Kim, J. Kim and J. Y. Lee, *Chem. Mater.*, 2020, **32**, 2583–2592.
8 H. Chen, Y. Deng, X. Zhu, L. Wang, L. Lv, X. Wu, Z. Li, Q. Shi, A. Peng, Q. Peng, Z. Shuai, Z. Zhao, H. Chen and H. Huang, *Chem. Mater.*, 2020, **32**, 4038–4044.
9 S. Reineke, F. Lindner, G. Schwartz, N. Seidler, K. Walzer, B. Lüssem and K. Leo, *Nature*, 2009, **459**, 234–238.
10 X. Wu, C. Y. Huang, D. G. Chen, D. Liu, C. Wu, K. J. Chou, B. Zhang, Y. Wang, Y. Liu, E. Y. Li, W. Zhu and P. T. Chou, *Nat. Commun.*, 2020, **11**, 2145.
11 Y. Kawamura, K. Goushi, J. Brooks, J. J. Brown, H. Sasabe and C. Adachi, *Appl. Phys. Lett.*, 2005, **86**, 0711104.
12 S. Hirata, *Adv. Opt. Mater.*, 2017, **5**, 1700116.
13 C. C. Kenry and B. Liu, *Nat. Commun.*, 2019, **10**, 2111.
14 B. Ding, L. Ma, Z. Huang, X. Ma and H. Tian, *Sci. Adv.*, 2021, **7**, eabf9668.
15 S. K. Lower and M. A. EL-Sayed, *Chem. Rev.*, 1966, **66**, 199.
16 N. Notsuka, R. Kabe, K. Goushi and C. Adachi, *Adv. Funct. Mater.*, 2017, **27**, 1703902.
17 K. Narushima, Y. Kiyota, T. Mori, S. Hirata and M. Vacha, *Adv. Mater.*, 2019, **31**, 1807268.
18 Q. Li, Y. Tang, W. Hu and Z. Li, *Small*, 2018, **14**, 1801560.
19 L. Gu, H. Shi, L. Bian, M. Gu, K. Ling, X. Wang, H. Ma, S. Cai, W. Ning, L. Fu, H. Wang, S. Wang, Y. Gao, W. Yao, F. Huo, Y. Tao, Z. An, X. Liu and W. Huang, *Nat. Photonics*, 2019, **13**, 406–411.
20 M. S. Kwon, D. Lee, S. Seo, J. Jung and J. Kim, *Angew. Chem., Int. Ed.*, 2014, **53**, 11177–11181.
21 Y. Wang, J. Yang, Y. Tian, M. Fang, Q. Liao, L. Wang, W. Hu, B. Z. Tang and Z. Li, *Chem. Sci.*, 2020, **11**, 833–838.
22 T. Wang, Z. Hu, X. Nie, L. Huang, M. Hui, X. Sun and G. Zhang, *Nat. Commun.*, 2021, **12**, 1364.
23 H. T. Feng, J. Zeng, P. A. Yin, X. D. Wang, Q. Peng, Z. Zhao, J. W. Y. Lam and B. Z. Tang, *Nat. Commun.*, 2020, **11**, 2617.
24 X. Zhang, L. Du, W. Zhao, Z. Zhao, Y. Xiong, X. He, P. F. Gao, P. Alam, C. Wang, Z. Li, J. Leng, J. Liu, C. Zhou, J. W. Y. Lam, D. L. Phillips, G. Zhang and B. Z. Tang, *Nat. Commun.*, 2019, **10**, 5161.
25 Z. Lin, R. Kabe, K. Wang and C. Adachi, *Nat. Commun.*, 2020, **11**, 191.
26 X. Wang, Y. Sun, G. Wang, J. Li, X. Li and K. Zhang, *Angew. Chem., Int. Ed.*, 2021, **60**, 17138–17147.
27 Y. Jie, S. Wang, Y. Ji, R. Chen, Q. Zhu, Y. Wang, C. Zheng, Y. Tao, Q. Fan and W. Huang, *Mater. Horiz.*, 2019, **6**, 1259–1264.
28 X. F. Wang, W. J. Guo, H. Xiao, Q. Z. Yang, B. Chen, Y. Z. Chen, C. H. Tung and L. Z. Wu, *Adv. Funct. Mater.*, 2020, **30**, 1907282.
29 P. She, Y. Yu, Y. Qin, Y. Zhang, F. Li, Y. Ma, S. Liu, W. Huang and Q. Zhao, *Adv. Opt. Mater.*, 2020, **8**, 1901437.
30 H. Shi, L. Song, H. Ma, C. Sun, K. Huang, A. Lv, W. Ye, H. Wang, S. Cai, W. Yao, Y. Zhang, R. Zheng, Z. An and W. Huang, *J. Phys. Chem. Lett.*, 2019, **10**, 595–600.
31 E. Hamzehpoor and D. F. Perepichka, *Angew. Chem., Int. Ed.*, 2019, **58**, 1–6.
32 J. Wang, Z. Huang, X. Ma and H. Tian, *Angew. Chem., Int. Ed.*, 2020, **59**, 1–7.
33 Z. Lin, R. Kabe, N. Nishimura, K. Jinnai and C. Adachi, *Adv. Mater.*, 2018, **30**, 1803713.
34 T. Ogoshi, H. Tsuchida, T. Kakuta, T. a. Yamagishi, A. Taema, T. Ono, M. Sugimoto and M. Mizuno, *Adv. Funct. Mater.*, 2018, **28**, 1707369.
35 H. A. Al-Attar and A. P. Monkman, *Adv. Funct. Mater.*, 2012, **22**, 3824–3832.
36 S. Guo, W. Dai, X. Chen, Y. Lei, J. Shi, B. Tong, Z. Cai and Y. Dong, *ACS Mater. Lett.*, 2021, **3**, 379–397.
37 J. Wei, B. Liang, R. Duan, Z. Cheng, C. Li, T. Zhou, Y. Yi and Y. Wang, *Angew. Chem., Int. Ed.*, 2016, **55**, 15589–15593.
38 Y. Wang, J. Yang, M. Fang, Y. Yu, B. Zou, L. Wang, Y. Tian, J. Cheng, B. Z. Tang and Z. Li, *Matter*, 2020, **3**, 449–463.
39 Y. Lei, W. Dai, J. Guan, S. Guo, F. Ren, Y. Zhou, J. Shi, B. Tong, Z. Cai, J. Zheng and Y. Dong, *Angew. Chem., Int. Ed.*, 2020, **59**, 16054–16060.
40 S. Hirata, *J. Phys. Chem. Lett.*, 2018, **9**, 4251–4259.
41 Y. Wang, S. Tang, Y. Wen, S. Zheng, B. Yang and W. Z. Yuan, *Mater. Horiz.*, 2020, **7**, 2105–2112.
42 M. Li, X. Cai, Z. Qiao, K. Liu, W. Xie, L. Wang, N. Zheng and S. J. Su, *Chem. Commun.*, 2019, **55**, 7215–7218.
43 X. Cai, Z. Qiao, M. Li, X. Wu, Y. He, X. Jiang, Y. Cao and S.-J. Su, *Angew. Chem., Int. Ed.*, 2019, **58**, 13522–13531.
44 S. Zheng, T. Hu, X. Bin, Y. Wang, Y. Yi, Y. Zhang and W. Z. Yuan, *ChemPhysChem*, 2019, **20**, 1–8.
45 L. Xiao and H. Fu, *Chem.–Eur. J.*, 2018, **24**, 1–11.
46 Q. Li and Z. Li, *Acc. Chem. Res.*, 2020, **53**, 962–973.
47 S. Hirata, K. Totani, J. Zhang, T. Yamashita, H. Kaji, S. R. Marder, T. Watanabe and C. Adachi, *Adv. Funct. Mater.*, 2013, **23**, 3386–3397.
48 H. Ma, W. Shi, J. Ren, W. Li, Q. Peng and Z. Shuai, *J. Phys. Chem. Lett.*, 2016, **7**, 2893–2898.
49 D. Beljonne, Z. Shuai, G. Pourtois and J. L. Bredas, *J. Phys. Chem. A*, 2001, **105**, 3899–3907.
50 K. Aidas, C. Angeli, K. L. Bak, V. Bakken, R. Bast, L. Boman, O. Christiansen, R. Cimiraglia, S. Coriani, P. Dahle,

E. K. Dalskov, U. Ekstrom, T. Enevoldsen, J. J. Eriksen, P. Ettenhuber, B. Fernandez, L. Ferrighi, H. Fliegl, L. Frediani, K. Hald, A. Halkier, C. Hattig, H. Heiberg, T. Helgaker, A. C. Hennum, H. Hettema, E. Hjertenaes, S. Host, I. M. Hoyvik, M. F. Iozzi, B. Jansik, H. J. Jensen, D. Jonsson, P. Jorgensen, J. Kauczor, S. Kirpekar, T. Kjaergaard, W. Klopper, S. Knecht, R. Kobayashi, H. Koch, J. Kongsted, A. Krapp, K. Kristensen, A. Ligabue, O. B. Lutnaes, J. I. Melo, K. V. Mikkelsen, R. H. Myhre, C. Neiss, C. B. Nielsen, P. Norman, J. Olsen, J. M. Olsen, A. Osted, M. J. Packer, F. Pawlowski, T. B. Pedersen, P. F. Provasi, S. Reine, Z. Rinkevicius, T. A. Ruden, K. Ruud, V. V. Rybkin, P. Salek, C. C. Samson, A. S. de Meras, T. Saue, S. P. Sauer, B. Schimmelpfennig, K. Sneskov, A. H. Steindal, K. O. Sylvester-Hvid, P. R. Taylor, A. M. Teale, E. I. Tellgren, D. P. Tew, A. J. Thorvaldsen, L. Thogersen, O. Vahtras, M. A. Watson, D. J. Wilson, M. Ziolkowski and H. Agren, *Wiley Interdiscip. Rev.: Comput. Mol. Sci.*, 2014, **4**, 269–284.

51 K. Burke, J. Werschnik and E. K. Gross, *J. Chem. Phys.*, 2005, **123**, 62206.

52 D. Kim, V. Coropceanu and J.-L. Brédas, *J. Am. Chem. Soc.*, 2011, **133**, 17895–17900.

53 P. Leoni, M. Pesquali and C. A. Ghilardi, *J. Chem. Soc., Chem. Commun.*, 1983, 240–241.

54 A. Yokoyama, A. Kato, R. Miyakoshi and T. Yokozawa, *Macromolecules*, 2008, **41**, 7271–7273.

55 Y. Lei, J. Yang, W. Dai, Y. Lan, J. Yang, X. Zheng, J. Shi, B. Tong, Z. Cai and Y. Dong, *Chem. Sci.*, 2021, **12**, 6518–6525.